REMARKS

Status of the Claims

Claims 1, 2, 5, 6, and 12-19 are pending in the present application. Claims 3, 4, and 7-11 were previously canceled.

Issues Under 35 U.S.C. § 112, Enablement

Claims 1-3, 5, 6, and 12-19 remain rejected under 35 U.S.C. § 112, first paragraph, as allegedly failing to comply with the enablement requirement.

Applicants traversed this rejection in the reply filed on June 29, 2009, providing arguments refuting the Examiner's contention. Applicants submit herewith further arguments and evidence, which supports the enablement of the instant claims.

Claim 3 was canceled in the June 29, 2009, response. Accordingly, the rejection is moot in regard to this claim.

In the interview of February 6, 2009, the Examiner stated that the present application and Figure 29 is insufficient to demonstrate that GANP transgenic mouse-derived hybridoma clones generate high-affinity antibodies. Specifically, the Examiner stated that Figure 29 only shows a single control. The Examiner further stated that if Applicants could provide additional data, which demonstrate that the controls cluster near W2-7 in Figure 29, such controls would support that the instant hybridoma clones produce high affinity antibodies.

Applicants previously noted in the June 29, 2009, response that Figure 29 demonstrates that high-affinity antibodies are generated using GANP transgenic mouse-derived hybridoma clones. The affinity of antibodies, generated after immunization with NP-CG antigen, *i.e.*, anti-NP antibody, was evaluated based upon the ability of the antibodies to bind to NP2-BSA, *i.e.*, two NPs coupled to BSA per molecule and NP17-BSA, *i.e.*, seventeen NPs coupled to BSA per molecule. Specifically, in ELISA analysis, the higher the value of NP2/NP17, (*i.e.*, the ability to bind to NP2-BSA/the ability to bind to NP17-BSA), the stronger the strength of binding to NP2-BSA, and, accordingly, the higher the affinity to the NP group. The results in Figure 29 show that the GANP transgenic mouse-derived hybridoma clones have higher affinity to the antigen compared to wild-type mouse-derived hybridoma clones. Applicants further submitted that the

control value, which describes a hybridoma derived from wild-type mouse, in conjunction with the disclosure in the present application, is sufficient evidence for an ordinary artisan to have recognized that the claimed transgenic mammals, parts thereof, and cells thereof, produce high affinity antibodies.

Notwithstanding the foregoing, Applicants would like to further direct the Examiner's attention to Figure 28 in the present application. Figure 28 depicts the results obtained after two wild-type and GANP transgenic mice were immunized with 100 μg/ml of NP-CG. At day 28, after the immunization, serum samples were taken from them and subjected to ELISA. As is evident from the Figure, the transgenic mice generated antibodies with much higher affinity against NP-CG in comparison to wild-type mice. Applicants submit that the controls used in Figures 28 and 29 are sufficient to allow an ordinary artisan to recognize that the claimed transgenic non-human mammals, parts thereof, and cells thereof, produce high affinity antibodies.

Applicants further submit herewith a journal article authored by the inventor and others, which was published subsequent to the international filing date of the instant application, *i.e.*, Sakaguchi *et al.*, *The Journal of Immunology*, 2005, 174:4485-4494. This peer reviewed journal article concludes that the transgenic mice described therein, which were prepared according to the methods described in the instant application, are capable of producing high affinity antibodies, *see*, *e.g.*, abstract. Further, the results depicted in Figure 28 are described in Figure 1*H* in the Sakaguchi *et al.*, publication. The Sakaguchi *et al.*, article states that [a]ffinity measurement with NP-hapten clearly demonstrated the high affinity of mAbs generated from the *Ganp*^{Tg} mice, *see* Sakaguchi *et al.*, page 4493, left column, first full paragraph. Applicants submit that the Sakaguchi *et al.* article further supports that the guidance in the present application is sufficient to allow an ordinary artisan to recognize that the claimed transgenic non-human mammals, parts thereof and cells thereof produce high affinity antibodies.

Based upon the foregoing and the response filed on June 29, 2009, Applicants submit that the present application enables the instant claims. Accordingly, withdrawal of the rejection is respectfully requested.

CONCLUSION

In view of the above remarks, applicant believes the pending application is in condition for allowance.

Should there be any outstanding matters that need to be resolved in the present application, the Examiner is respectfully requested to contact Linda T. Parker Reg. No. 46,046 at the telephone number of the undersigned below, to conduct an interview in an effort to expedite prosecution in connection with the present application.

If necessary, the Commissioner is hereby authorized in this, concurrent, and future replies to charge payment or credit any overpayment to Deposit Account No. 02-2448 for any additional fees required under 37.C.F.R. §§1.16 or 1.17; particularly, extension of time fees.

Dated: JUL 23 2009

Respectfully submitted,

By _____
Gerald M. Murphy, Jr.
Registration No.: 28,977
BIRCH, STEWART, KOLASCH & BIRCH, LLP
8110 Gatehouse Road
Suite 100 East
P.O. Box 747
Falls Church, Virginia 22040-0747
(703) 205-8000
Attorney for Applicant

Enclosures: Sakaguchi *et al.*, *The Journal of Immunology*, 2005, 174:4485-4494

Generation of High-Affinity Antibody against T Cell-Dependent Antigen in the *Ganp* Gene-Transgenic Mouse[1]

Nobuo Sakaguchi,[2]*¶ Tetsuya Kimura,[†] Shuzo Matsushita,[†] Satoru Fujimura,* Junji Shibata,[†] Masatake Araki,[‡] Tamami Sakamoto,[§] Chiemi Minoda,[§] and Kazuhiko Kuwahara*‖

Generation of high-affinity Ab is impaired in mice lacking germinal center-associated DNA primase (GANP) in B cells. In this study, we examined the effect of its overexpression in *ganp* transgenic C57BL/6 mice (*Ganp*^{Tg}). *Ganp*^{Tg} displayed normal phenotype in B cell development, serum Ig levels, and responses against T cell-independent Ag; however, it generated the Ab with much higher affinity against nitrophenyl-chicken gammaglobulin in comparison with C57BL/6. To further examine the affinity increase, we established hybridomas producing high-affinity mAbs and compared their affinities using BIAcore. C57BL/6 generated high-affinity anti-nitrophenyl mAbs (K_D ~ 2.50 × 10^{-7} M) of IgG1/λ1 and contained the V_H*186.2* region with W33L mutation. *Ganp*^{Tg} generated much higher affinity (K_D > 1.57 × 10^{-9} M) by usage of V_H*186.2* as well as noncanonical V_H*7183* regions. *Ganp*^{Tg} also generated exceptionally high-affinity anti-HIV-1 (V3 peptide) mAbs (K_D > 9.90 × 10^{-11} M) with neutralizing activity. These results demonstrated that GANP is involved in *V* region alteration generating high-affinity Ab. *The Journal of Immunology*, 2005, 174: 4485–4494.

The Ag-driven B cells expressing high-affinity BCR, which have been selected in secondary lymphoid organs, generate high-affinity Ab. Ag-driven B cells proliferate rapidly by the stimulation with Ag and costimulatory molecules from Th cells surrounding the germinal center (GC)[3] region, in which such B cells undergo affinity maturation of Ig V region and class switching of the C region during the response to T cell-dependent Ag (TD-Ag) in vivo (1, 2). For affinity maturation, introduction of somatic hypermutation (SHM) in the *V* region is probably essential and, in addition to this molecular alteration, the Ag-driven B cells with high-affinity BCR must be selected or further enriched during the maturation of Ag-driven B cells in GCs.

A 210-kDa germinal center-associated DNA primase (GANP) protein, bearing RNA-primase and minichromosome maintenance (MCM)3-binding activities, is up-regulated in GC B cells upon immunization with TD-Ag in vivo and is induced by the stimulation to BCR and CD40 in vitro (3, 4). The mutant mouse with *ganp* gene knockout B cells (B-*ganp*$^{-/-}$) has a severe defect in mounting high-affinity Ab responses to TD-Ag (5), suggesting that GANP is required for generation of high-affinity Ab in response to TD-Ag in vivo. However, there remained several possibilities to account for the molecular mechanism in generation of high-affinity V regions by the expression of GANP in GC B cells. GANP might augment the induction of SHM in the *V* regions, resulting in the affinity maturation of V regions during the proliferation and differentiation of Ag-driven B cells in GCs. Alternatively, GANP might be involved in the survival of the high-affinity BCR$^+$ B cells for the positive selection through the interaction of Ags captured on the follicular dendritic cell network. The GCs of the B-*ganp*$^{-/-}$ mice displayed an increase of apoptotic cells upon immunization with TD-Ag SRBC, which suggested a partial involvement of GANP in the survival of GC B cells. However, the *ganp*$^{-/-}$ B cells do not show marked abnormalities in the levels of apoptotic and proapoptotic molecules after BCR cross-linkage (5). To study the function of GANP in generation of high-affinity Ab response, it is necessary to examine whether the affinity maturation of BCR on the GC B cell is generated by the genetic alteration in the *V* region gene.

We speculated that it would be possible to generate a high-affinity Ab if we used mice with higher level GANP expression in B cells. We studied whether the transgenic mouse with increased expression of *ganp* gene could generate high-affinity Ab against TD-Ag using a model epitope of 4-hydroxy-3-nitrophenyl acetyl (NP)-hapten in the C57BL/6 background. To demonstrate the increased affinity of the Ab in detail, we established the hybridomas secreting anti-NP mAbs after immunization with NP-chicken gammaglobulin (CG) in *Ganp*^{Tg} mice. After selecting the high-affinity mAbs against NP-hapten by differential ELISA method and the BIAcore system, we examined the *V* region gene usage of the hybridomas and compared the sequences with those from wild-type C57BL/6 mice. The results suggest that the affinity maturation of BCR on GC B cells is generated by the altered V_H region usage with increased SHM in *Ganp*^{Tg} mice.

Materials and Methods

Ganp^{Tg} *mouse*

The expression construct of mouse *ganp* cDNA under the mouse Ig promoter and human Ig enhancer (6) was used for establishing the transgenic

*Department of Immunology, Graduate School of Medical Sciences, [†]Division of Clinical Retrovirology and Infectious Diseases, Center for AIDS Research, [‡]Division of Bioinformatics, Institute of Resource Development and Analysis, Kumamoto University, and [§]Trans Genic, Kumamoto Japan; [¶]Core Research for Evolutional Science and Technology Program, Saitama Japan; and [‖]PRESTO, Japan Science and Technology Agency, Saitama, Japan

Received for publication October 26, 2004. Accepted for publication January 4, 2005.

The costs of publication of this article were defrayed in part by the payment of page charges. This article must therefore be hereby marked *advertisement* in accordance with 18 U.S.C. Section 1734 solely to indicate this fact.

[1] This work was supported by Special Coordination Funds for Promoting Science and Technology from the Ministry of Education, Culture, Sports, Science and Technology of Japan, Matching Funds from New Energy and Industrial Technology Development Organization, and grants from the Core Research for Evolutional Science and Technology Program, Japan Science and Technology Agency.

[2] Address correspondence and reprint requests to Dr. Nobuo Sakaguchi, Department of Immunology, Graduate School of Medical Sciences, Kumamoto University, 1-1-1, Honjo, Kumamoto 860-8556, Japan. E-mail address: nobusaka@kaiju.medic.kumamoto-u.ac.jp

[3] Abbreviations used in this paper: GC, germinal center; GANP, germinal center-associated DNA primase; NP, 4-hydroxy-3-nitrophenyl acetyl; SHM, somatic hypermutation; TD-Ag, T cell-dependent Ag; MCM, minichromosome maintenance; CG, chicken gammaglobulin; KLH, keyhole limpet hemocyanin; TNP, 2,4,6-trinitrophenyl; LTR, long terminal repeat.

0022-1767/05/$02.00

mouse by the standard procedure. Mice were screened for the transgene by PCR using *ganp* 1–5′ primer (5′-TCCCGCCTTCCAGCTGTGAC-3′) and *ganp* 1–3′ primer (5′-GTGCTGCTGTGTTAT GTCCT-3′) and Southern blot analysis using *ganp* probe A (1143–2193 nt) of tail genomic DNAs. The *Ganp*^{Tg} mice that express 1.5- to 2.0-fold increase of *ganp* gene grew normally under specific pathogen-free condition and were immunized with Ags. *Ganp* transcripts were detected by two primers (*ganp* 1–5′ and *ganp* 1–3′) in comparison with *β-actin* control (5). All mice were maintained in the Center for Animal Resources and Development (Kumamoto University, Kumamoto, Japan).

Flow cytometric analysis

Single-cell suspensions from lymphoid organs were stained with each biotin-labeled mAb in combination with FITC-conjugated streptavidin (Amersham Biosciences) and PE-conjugated mAbs. Lymphoid cells were analyzed by FACSCalibur (BD Biosciences) using CellQuest software.

In vitro proliferation assay

Purified B cells were cultured for 48 h at a density of 2×10^5 cells/well in 96-well microtiter plates in RPMI 1640 medium containing 10% heat-inactivated FCS (JRH Biosciences), 2 mM L-glutamine, and 5×10^{-5} M 2-ME. The cells stimulated with or without various mitogenic stimulants were pulsed with 0.2 μCi/well of [^{3}H]thymidine (ICN Pharmaceuticals) for 16 h before harvesting, and the incorporated radioactivity was measured by scintillation counter. Stimulatory reagents were affinity-purified goat anti-mouse μ-chain-specific Ab (F(ab′)$_2$, 10 μg/ml; ICN Pharmaceuticals), rat anti-mouse CD40 mAb (LB429, 10 μg/ml) (4), and LPS (10 μg/ml; Sigma-Aldrich).

Immunohistochemistry

The 8-μm sections of spleen from SRBC-immunized mice were lightly fixed with acetone. Slides were blocked with 3% BSA in PBS-Tween 20

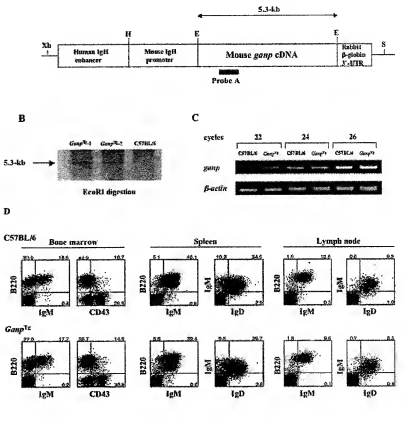

FIGURE 1. Generation of transgenic mice that overexpress the *ganp* gene in B cells. *A*, A schematic diagram of construct for *Ganp*^{Tg} under the human Ig enhancer, mouse Ig promoter, and followed by rabbit β-globin 3′-untranslated region (UTR). The construct contains restriction enzyme sites: Xb, *Xba*I; H, *Hind*III; E, *Eco*RI; and S, *Sal*I. The probe for Southern blot analysis (probe A) is indicated. *B*, Detection of the *ganp* transgene by Southern blot analysis. Southern blot analysis with *Eco*RI-digested genomic DNAs of *Ganp*^{Tg} displayed a 5.3-kb band hybridized with probe A. *C*, Up-regulation of *ganp* transcripts in B cells from *Ganp*^{Tg}. Semiquantitative PCR was performed using the primers *ganp* 1–5′ and *ganp* 1–3′, in comparison with *β-actin* transcripts. From densitometer analysis, *ganp* transcripts in B cells from *Ganp*^{Tg} showed an 80% increase in comparison with C57BL/6 mice. *D*, Flow cytometric analysis. Bone marrow, spleen, and lymph node cells from 8-wk-old C57BL/6 and *Ganp*^{Tg} were analyzed with indicated markers. *E*, In vitro proliferation assay of purified B cells from *Ganp*^{Tg}. [^{3}H]Thymidine incorporation was measured in the presence or absence of B cell mitogenic stimulants in C57BL/6 mice (■) and *Ganp*^{Tg} mice (□). The representative data are shown from four independent experiments. *, $p < 0.05$. *F*, Kinetics of GC formation after TD-Ag in *Ganp*^{Tg}. C57BL/6 and *Ganp*^{Tg} mice were immunized by SRBC. At day 10 or day 14, the sections were doubly immunostained with peanut agglutinin (brown) and IgD (blue). Arrows indicate GCs. *G*, T cell-indepndent Ag (type II)-specific or TD-Ag-specific immune responses in *Ganp*^{Tg}. Sera from mice immunized with TNP-Ficoll or TNP-KLH were collected at day 14. TNP-specific Ab titers were measured by ELISA. C57BL/6 mice (●) and *Ganp*^{Tg} mice (○) are indicated. *H*, Relative affinity of serum Abs in *Ganp*^{Tg}. Sera from C57BL/6 and *Ganp*^{Tg} mice immunized with NP-CG were collected at days 14 and 28. The NP_2 to NP_{17} ratios of anti-NP IgG1 were measured by ELISA. *I*, W33L mutation of $V_H186.2$ transcripts from C57BL/6 and *Ganp*^{Tg} mice. Mice were i.p. immunized by 20 μg of alum-precipitated NP-CG. $V_H186.2$ transcripts of γ1-isotype were amplified by RT-PCR and cloned into pBluescript vector for sequencing. The calculated percentage from sequence data was shown in C57BL/6 (■) and *Ganp*^{Tg} (□) mice. *, $p < 0.05$.

FIGURE 1. (*continues*)

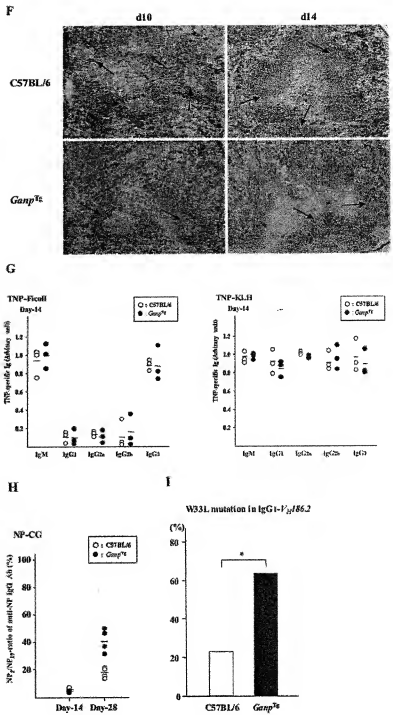

FIGURE 1. *continued.*

and incubated with anti-IgD mAb in combination with alkaline phosphatase-conjugated anti-rat IgG (ICN Pharmaceuticals). The first development step was conducted with Vector Blue kit (Vector Laboratories). For second staining, slides were incubated with biotin-conjugated peanut agglutinin (Vector Laboratories) in combination with HRP-conjugated streptavidin (Kirkegaard & Perry Laboratories), followed by 3,3′-diaminobenzidine tetrahydrochloride (Dojindo). After fixation with 1% glutaraldehyde in PBS, mounting was done by Aquatex (Merck).

Ag and immunization

2,4,6-Trinitrophenyl (TNP)-keyhole limpet hemocyanin (KLH), TNP-Ficoll, and NP_{28}-CG were purchased from Biosearch Technologies. From 20 to 100 μg of TNP-KLH and NP-CG precipitated by alum (Pierce), or 25 μg of TNP-Ficoll dissolved in PBS was injected i.p. into C57BL/6 and *Ganp*^{Tg} mice.

Measurement of Ag-specific Ab production

Five micrograms per well of TNP-BSA (Biosearch Technologies) were coated on ELISA plate, blocked with 3% BSA in PBS, and incubated with the serial-diluted sera obtained at day 14 after Ag immunization. After washing with PBS-0.1% Tween 20, the wells were incubated with biotin-conjugated isotype-specific mAb in combination with alkaline phosphatase-conjugated streptavidin (Southern Biotechnology Associates). The development was performed in the presence of substrate.

Sequence analysis of $V_H186.2$ gene

The *Ganp*^{Tg} mice were immunized with alum-precipitated NP-CG once as described (5). After 28 days, the spleen B cells were purified, and the total

Table 1. *Affinity of the anti-NP mAb measured by BIAcore sensorgram*

mAb	H Chain	L Chain	V_H Usage	K_D, M[a]
Ganp^{Tg}				
NP-G2–6	γ1	κ	V_H 7183 family	7.05×10^{-8}
NP-G2–9	γ1	κ	V_H 7183 family	3.24×10^{-8}
NP-G2–12	γ1	λ	V_H 186.2	4.92×10^{-8}
NP-G2–14	γ1	κ	V_H 186.2	2.51×10^{-8}
NP-G2–16	γ2b	λ	V_H 186.2	1.10×10^{-7}
NP-G2–15	γ1	λ	V_H 186.2	4.12×10^{-8}
NP-G-2E4	γ2b	λ	V_H 186.2	1.57×10^{-9}
C57BL/6				
NP-W2–7	γ1	λ	V_H 186.2	1.51×10^{-7}
NP-W1–116	γ2a	λ	V_H 186.2	1.00×10^{-8}
NP-W-1B9	γ2b	λ	V_H 186.2	1.24×10^{-8}
NP-W-2D8	γ2b	λ	V_H 186.2	2.74×10^{-8}

[a] K_D was calculated using BIAcore sensorgram as described in *Materials and Methods*.

RNA was used for RT-PCR analysis with the sequence primers for IgG1-V_H*186.2* and the sequences were compared with those of C57BL/6.

Establishment of mAbs

Ag immunization was conducted with CFA as a primary immunization and then followed by boosting with IFA (4). For anti-NP-specific mAbs, NP_{28}-CG emulsified in CFA was injected i.p. and boosted after 2 wk with IFA. The mice with higher serum Ab titers were further immunized, and 3 days later, the spleen cells were obtained for cell fusion by polyethylene glycol method with mouse myeloma cell line X63 under the standard procedure (4). The fused cells were selected with hypoxanthine/aminopterin/thymidine medium on the microculture plates at the concentration of 2×10^4 cells/well with IL-6 (5 U/ml). For preparation of mAbs against the epitope of HIV-1, the peptide of the CNNTRKSIRIQRGPGRAFVYIGKI was prepared based on the amino acid sequence of the V3 loop of gp120 region of NL4-3 HIV-1 strain (prototype X4; T cell tropic) and conjugated with KLH (Merck). Sera of immunized mice were measured by ELISA using the plates coated with the HIV-1 peptide conjugated with BSA.

ELISA screening

For anti-NP mAbs, supernatants of individual wells were divided into two aliquots (each 50 μl) and measured by the differential ELISA method with two different Ag-coating as NP_2-BSA and NP_{17}-BSA (Biosearch Technologies) under the standard procedure. The mAbs binding to the Ags were captured with protein A-peroxidase (Amersham Biosciences) with the substrate (Bio-Rad). The positive signals with NP_2-BSA plates were selected in comparison with NP_{17}-BSA plates. The mAbs showing little difference (NP_2-BSA/NP_{17}-BSA > 0.5) between the two plates were cloned by limiting dilution method. Then, the positive clones were expanded for large scale to purify the mAbs in the serum-free medium (Invitrogen Life Technologies) and the mAbs were purified through protein G-Sepharose column chromatography (Amersham Biosciences) and the protein concentrations were determined by Bradford assay kit (Bio-Rad). The purities of the samples were examined by SDS-PAGE and the protein staining with Coomassie brilliant blue. The isotypes of H chain and L chain in all mAbs were determined by Isotyping kit (Dainippon Pharmaceuticals).

BIAcore assay

Affinity of the mAbs was determined by the BIAcore assay (7). The on and off rate constants (k_{on} and k_{off}) for binding of the mAbs to NP or HIV-1 V3 loop peptide were determined by BIAcore system (Biacore International). The carboxyl-methylated dextran surface of the sensor chip was activated with EDC (*N*-ethyl-*N*′-(3-dimethylaminopropyl)carbodiimide) and NHS (*N*-hydroxysuccinimide) (8). V3 loop peptide was immobilized through the free thiol group of a cysteine residue that was deliberately placed at the N terminus, by injection of 35 μl of a 20 μg/ml solution in 10 mM MES buffer (pH 6) to the EDC-NHS-activated surface that had been reacted with 2-(2-pyridinyldithio)ethaneamine. The excess disulfide groups were deactivated by the addition of cysteine. The mAbs were diluted in 10 mM HEPES (pH 7.4), 150 mM NaCl, 3.4 mM EDTA, and 0.05% (v/v) BIAcore surfactant P20 and injected over the immobilized Ag at a flow rate of 5 μl/min. The association was monitored by the increase of the refractive index of the sensor chip surface per unit time. The dissociations of the mAbs were monitored after the end of the association phase with a flow rate of 50 μl/min. Kinetic rate constants were calculated from the collected data using the Pharmacia Kinetics Evaluation software (9). The k_{on} was determined by measuring the rate of binding to the Ag at different protein concentrations.

DNA sequencing

The DNA fragments corresponding to the rearranged V_H regions were amplified using Pfu-Turbo (Stratagene) from the genomic DNA. The oligonucleotide primers are as follows (10, 11): V_H186.2 forward, 5′-CTGAC CCATGTCCCTCTTCTCTCCAGCAGG-3′; V_H7183 forward, 5′-GCA GCTGGTGGAGTCTGG-3′; J_H4-3, 5′-CTCTCAGCCGGCTCCCTCA GGG-3′; VA1 forward, 5′-TGCTGACCAATATTGAAAAG-3′; JA1 reverse, 5′-AGCACCTCAAGTCTTGGAGAG-3′. For rearranged *V* κ-chain genes, the cDNA fragments were amplified using the primers designed as follows (12): V κ-Ox1 forward, 5′-ATGGATTTTCAAGTGCAGATTTTCA-3′; Vκ-21B forward, 5′-ATGGAGTCAGACACACTCCTGCTAT-3′; and Cκ reverse, 5′-TGGGAAGATGGATACAGTTGGTGCA-3′. Amplification of Cμ region was conducted with the primers: Cμ-Ex1 forward, 5′-AGTCAGTCCTTCCCAAATGTCTTCCC-3′ and Cμ-Ex3 reverse, 5′-TGAAGGTTAGGATGTCTGTGGAGGG-3′. The amplified DNA fragments cloned into blunt-ended pBluescript were sequenced.

In vitro binding assay to NLA-3 envelope

293T cells were transfected with pLP-IRES2 enhanced GFP (BD Clontech) or pLP-NL4-3 envelope enhanced GFP using Effectene Transfection Reagent (Qiagen). After 36 h, cells were harvested, incubated with each anti-HIV-1 mAb in combination with allophycocyanin-conjugated goat anti-mouse IgG Ab (BD Pharmingen), and analyzed in comparison with GFP expression by FACSCalibur. The anti-CD19 mAb was purchased from BD Biosciences.

Neutralization activity assay

HIV-1 strain NL4-3 (prototype X4; T cell tropic) was propagated in PM1 cells in RPMI 1640 medium with 10% (v/v) heat-inactivated FCS, and the cell-free supernatant was collected and stored as virus stocks at −80°C. The chemiluminescent assay (Galacto-Star; Applied Biosystems) for β-galactosidase released from the HeLa-CD4$^+$/long terminal repeat (LTR)-β-galactosidase/CCR5 (MAGI/CCR5) cells were conducted as previously described (13). Tissue culture-effective dose ($TCID_{50}$) of virus stock was predetermined with MAGI/CCR5 cells by the method of Reed and Muench (14). For the assay of neutralizing activity against HIV-1 infection, MAGI/CCR5 cells were plated in 96-well microtiter plates at a density of 1×10^4 cells/well, and on the next day, the cells were incubated with 50 μl of each mAb and 50 μl of HIV-1 solution (500 $TCID_{50}$) for 30 min at 37°C in combination with 10 μg/ml DEAE-dextran (Amersham Biosciences) in a triplicate assay. After 48 h, we measured the β-galactosidase activity for 1 s using the Galacto-Star system according to the manufacturer's protocol and showed results as percentages of the negative control.

Results

Establishment of Ganp^{Tg} *mice*

Ganp^{Tg} mice were established under control by human Ig enhancer and mouse Ig promoter in C57BL/6 background (Fig. 1, *A* and *B*), and the adult mice showed an increase of *ganp* transcripts (~2-fold) in B cells (Fig. 1*C*). *Ganp*^{Tg} mice had normal B lineage differentiation by surface marker studies of B220, IgM, and IgD on lymphoid cells in the bone marrow, spleen, and lymph nodes (Fig. 1*D*). B cell numbers and the levels of serum Igs were also normal in *Ganp*^{Tg} mice (data not shown). These results demonstrated that B cell differentiation undergoes normally in *Ganp*^{Tg} mice compared with wild-type littermates.

In vitro B cell proliferation and GC formation of Ganp^{Tg} *mice*

Next, we examined the potential of B cell proliferation of *Ganp*^{Tg} mice in vitro. *Ganp*^{Tg} mice showed comparable proliferation activities to wild-type littermates in response to anti-μ Ab, anti-μ Ab plus anti-CD40 mAb, or LPS (Fig. 1*E*). Interestingly, *Ganp*^{Tg} B cells showed augmented responses to anti-CD40 stimulation in comparison to wild-type B cells. This was only observed in the response to anti-CD40 stimulation but not in the response to anti-μ Ab or LPS stimulation, suggesting that *Ganp*^{Tg} mice augment CD40-stimulated response in vivo.

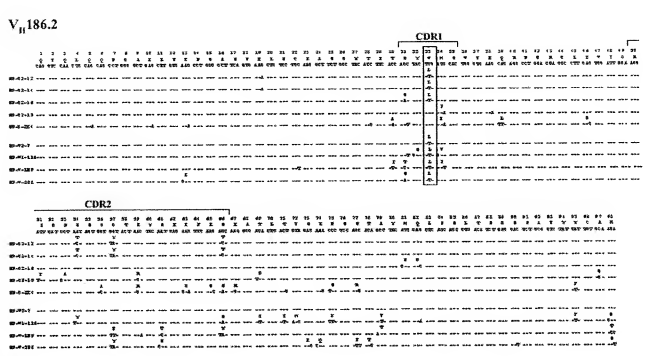

FIGURE 2. (*continues*)

We examined whether *Ganp*^{Tg} mice showed the alteration of GC formation in vivo. *Ganp*^{Tg} mice did not show any difference in the size and number of GCs at day 10 after SRBC immunization; however, in contrast to the findings observed in B-*ganp*$^{-/-}$ mice (4), *Ganp*^{Tg} mice showed the accelerated resolution of GC formation in vivo (Fig. 1*F*). This response could be due to the efficient production of high-affinity Ab in *Ganp*^{Tg} mice.

Responses of Ganp^{Tg} *mice against T cell-independent Ag and TD-Ag*

Because GANP expression is selectively up-regulated in GC B cells, we studied the Ab responses of *Ganp*^{Tg} mice. After Ag immunization, the responses were measured for T cell-independent type II Ag and TD-Ag at various time points and the results of day 14 were shown. The serum titers of Ag-specific Abs against TNP-Ficoll as T cell-independent Ag and TNP-KLH as TD-Ag were normal with similar distributions of various Ig isotypes in comparison with wild-type littermates (Fig. 1*G*).

Enhanced affinity maturation of Ganp^{Tg} *mice against TD-Ag*

However, after immunization with NP-CG, *Ganp*^{Tg} showed high affinity by the differential ELISA with the pauci NP_2-BSA conjugate that yielded 42% of the response to the multihapten NP_{17}-BSA conjugate in comparison with C57BL/6 (Fig. 1*H*). Jacob et al. (15, 16) showed that, in (NP-CG)-immunized C57BL/6 mice, the Abs in the secondary response against NP were exclusively IgG1/λ1 and had a single V_H region ($V_H186.2$) carrying with a peculiar pattern of mutation for high affinity. We investigated whether the affinity increase of anti-NP Ab generated in *Ganp*^{Tg} mice accompanied with the similar mutation pattern in the $V_H186.2$ locus. The $V_H186.2$ sequence was studied by RT-PCR using the spleen B cells from (NP-CG)-immunized mice. *Ganp*^{Tg} showed striking increases in mutation at ^{33}W to L of the $V_H186.2$ locus in splenic B cells (W33L; Fig. 1*I*). These results demonstrated that *Ganp*^{Tg} induced a higher frequency of the high-affinity mutation during the immune response to TD-Ag.

Establishment of hybridomas secreting high-affinity anti-NP-hapten

Anti-NP hybridomas were established by immunization of *Ganp*^{Tg} with NP-CG. Supernatants from >6000 clones were screened by the differential ELISA to identify wells with high-affinity mAbs, and the selected hybridoma cells were cloned. Affinities of those

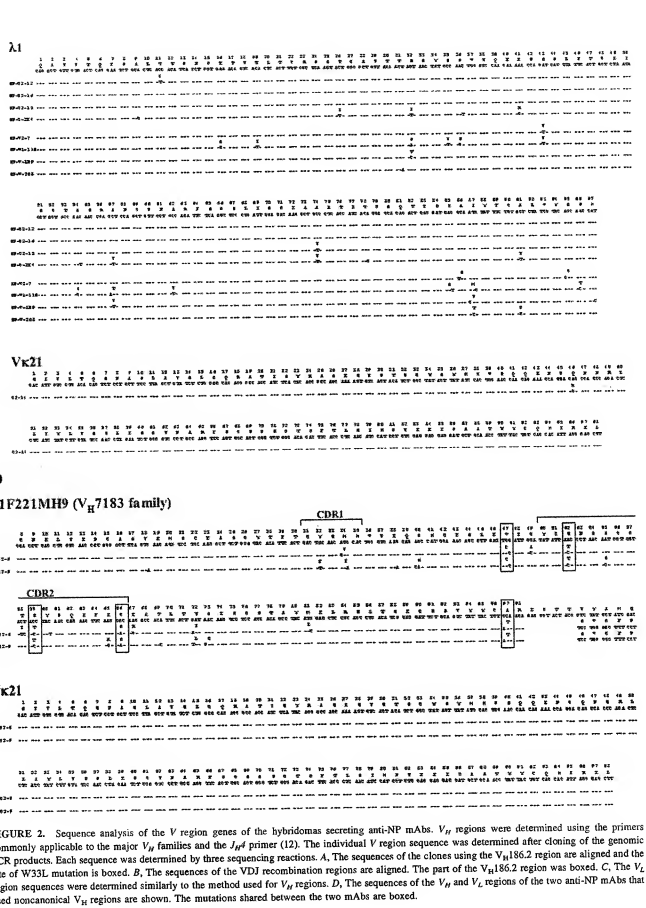

FIGURE 2. Sequence analysis of the *V* region genes of the hybridomas secreting anti-NP mAbs. V_H regions were determined using the primers commonly applicable to the major V_H families and the J_H#1 primer (12). The individual *V* region sequence was determined after cloning of the genomic PCR products. Each sequence was determined by three sequencing reactions. *A*, The sequences of the clones using the V_H186.2 region are aligned and the site of W33L mutation is boxed. *B*, The sequences of the VDJ recombination regions are aligned. The part of the V_H186.2 region was boxed. *C*, The V_L region sequences were determined similarly to the method used for V_H regions. *D*, The sequences of the V_H and V_L regions of the two anti-NP mAbs that used noncanonical V_H regions are shown. The mutations shared between the two mAbs are boxed.

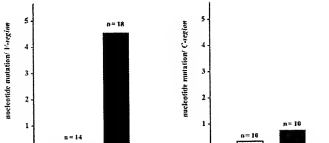

FIGURE 3. Mutation frequency induced in the V_H7183 family gene (C1F221MH9) by NP-CG immunization. NP-binding GC B cells were purified by a cell sorter 14 days after immunization with NP-CG in $Ganp^{Tg}$ and C57BL/6 mice. The V_H7183 family gene and $C\mu$ gene were PCR-amplified by Pfu-Turbo with genomic DNAs, cloned into TOPO cloning vector, and then sequenced. The mutation frequencies were counted based on the genomic sequences in the European Molecular Biology Laboratory database and were shown as average mutations per V_H region or $C\mu$ region sequences. The number (n) shows the V_H region (*left*) or $C\mu$ region (*right*) DNAs cloned in the TOPO cloning vector.

mAbs, after purification from clone culture supernatants, to NP-hapten were measured by the BIAcore system with a sensor chip conjugated with NP using Pharmacia Kinetics Evaluation software (9). The K_D of each mAb was determined by measuring the rate of binding to the Ag at different protein concentrations. The affinity of mAbs from (NP-CG)-immunized $Ganp^{Tg}$ and C57BL/6 mice were compared and the representatives were shown (Table I). The high-affinity mAbs of C57BL/6 mice used the $V_H186.2$ region in combination with λ1 L chain and yielded affinities from $K_D = 1.51 \times 10^{-7}$ M to 1.0×10^{-8} M. The mAbs from $Ganp^{Tg}$ showed the usage of canonical $V_H186.2$ in combination with both κ and λ yielding affinities from $K_D = 1.10 \times 10^{-7}$ M to 1.57×10^{-9} M. Interestingly, the mAbs from $Ganp^{Tg}$ also used noncanonical V_H region of V_H7183 family in combination κ-chain but showed similarly high affinities.

The usage and mutation of V *region genes in the anti-NP hybridomas*

The high-affinity mAbs obtained from C57BL/6 mice used the canonical $V_H186.2$ gene with the W33L mutation that is responsible for high affinity. This change increased the affinity from $K_D = 2 \sim 4 \times 10^{-6}$ M to 2×10^{-7} M (17, 18). The other mutations in the $V_H186.2$ gene segment would not have contributed to increased affinity against NP-hapten (19). Therefore, we sequenced the V_H regions of the hybridomas to examine whether there were similar mutation profiles of the V region. The mAbs from C57BL/6 mice generated typical high affinity against NP-hapten by using the $V_H186.2$ region with W33L mutation in combination with $DFL16.1$ and J_H2 gene segments. $Ganp^{Tg}$ generated similar high-affinity mAbs (NP-G2-12; $K_D = 4.92 \times 10^{-8}$, NP-G2-16; 1.10×10^{-7} M) (Table I) with the $V_H186.2$ having the W33L mutation (Fig. 2*A*). Interestingly, two anti-NP hybridomas that did not bear the W33L mutation in $V_H186.2$ showed similar high affinities. NP-G2-15 had the mutation of Y99G as reported previously (10). NP-G-2E4 with higher affinity ($K_D = 1.57 \times 10^{-9}$ M) did not have either of these two mutations but instead showed 13 aa mutations (22 nt changes) in the $V_H186.2$ region with the usage of $DSP2.6$ and J_H2 regions (Fig. 2, *A* and *B*). The L chain of NP-G-2E4 also had 6 aa mutations (10 nt changes) (Fig. 2*C*). This result suggested that the high affinity of NP-G-2E4 was generated by the extraordinarily increased V region mutations.

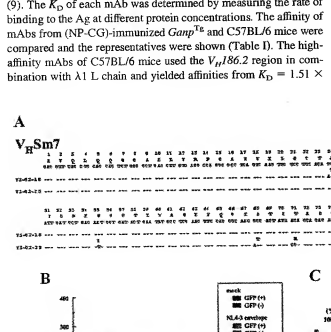

FIGURE 4. The sequences of the V_H region, the Ag-binding activities, and the neutralizing activities of the mAbs against the V3 epitope of HIV-1 gp120. *A*, The V_H region sequence (V_HSm7) used for the high-affinity mAbs from $Ganp^{Tg}$ is shown. The mutation site commonly observed in the two V_H sequences is boxed. *B*, Binding activity of the mAbs against HIV-1 envelope. Specific binding of the mAbs were shown as mean fluorescence intensity (MFI) examined with allophycocyanin-conjugated goat anti-mouse IgG Ab in combination with the NL4-3 envelope-expressing GFP^+-transfectants by using flow cytometry. Negative controls were measured with GFP^--mock transfectants. Another negative control for mAb binding was shown by CD19 mAb. *C*, Neutralizing activities were measured using a CD4-LTR/β-galactosidase-induced HeLa cell line. After $TCID_{50}$ of virus stock was predetermined with MAGI/CCR5 cells, the virus infection assay was conducted in vitro, to which anti-V3 epitope mAbs were added. Higher neutralization activities were significant (*) for the mAbs produced by $Ganp^{Tg}$ (V3-G2-10 and V3-G2-25) as compared with those of C57BL/6 mice at the concentration of 0.5 μg/mL. Negative control is shown with anti-CD19.

Moreover, two anti-NP mAbs from *Ganp*^{Tg} yielding similarly high affinities ($K_D = 3.24 \sim 7.05 \times 10^{-8}$ M) used noncanonical V_H region sequences, both of which probably originated from the same genomic *V_H7183* family. The best match in the Celera Discovery System was to the C1F221MH9 (*V_H7183* family), but the two clones showed variations with >12 nt differences from the genomic C1F221MH9 sequence (Fig. 2*D*). Mutations of W47C, N52C, S59T, G66D, and A97T were commonly observed in the V_H region (C1F221MH9), suggesting their contributions to raise the affinity of the mAb against NP-hapten. However, mutations in the V_L regions were not apparently increased in the comparison of the anti-NP mAbs from *Ganp*^{Tg} and C57BL/6 mice. The generation of high-affinity BCR without the exchange at position 33 is a rare event, which suggested that the combination of particular D-J_H sequences and/or many SHMs do not result in high affinity (18). A recent report only showed the case of mutation, Y99G in V_H186.2, which generated similar high-affinity mAb against NP-hapten comparable to W33L (10). Extensive earlier studies of anti-NP mAbs found that repeated immunization of C57BL/6 mice with NP-CG increased usage of noncanonical V_H regions and different L chain combinations (16). However, as far as we know, no study with conventional animals has demonstrated comparable high-affinity mAbs to those reported in this study. Although crystallographic studies are needed for definitive conclusions, we speculate that hypermutated C1F221MH9 V_H region (V_H7183 family) in association with other L chain combinations creates an effective tertiary structure for Ag-binding, yielding closer interactions of hypermutated C1F221MH9 V_H region and NP-hapten, and might be as effective as mAbs with the V_H186.2 region.

Mutations induced in the noncanonical V_H region of the spleen B cells after immunization with NP-CG

Usually wild-type C57BL/6 mice do not induce such a frequent mutation in the noncanonical V_H region in GC B cells before and after immunization with NP-CG. We examined the mutation frequency of the *V_H7183* family gene (C1F221MH9) under a non-immunization condition in spleen B cells of *Ganp*^{Tg} mice but found no alteration of the V_H region (data not shown). To study whether such hypermutation could be observed in *Ganp*^{Tg} spleen B cells after immunization, we investigated mutations in the *V_H7183* family gene (C1F221MH9) by examining genomic DNA of NP-binding GC B cells purified by cell sorting. These DNAs showed 16-fold higher mutation frequencies (4.5 mutations/V_H region of *Ganp*^{Tg} mAb vs 0.28 mutations/V_H region of C57BL/6 mAb) in the *V_H7183* family (Fig. 3, *left panel*). In contrast, such higher mutation frequencies were not observed in the Cμ region (Fig. 3, *right panel*). This is in agreement with the suggestion that *Ganp*^{Tg} has a high frequency of SHM that contributes to the production of high-affinity BCR in vivo. Alternatively, *Ganp*^{Tg} might effectively rescue and maintain B cells with high-affinity BCR during the immune response.

Establishment of high-affinity mAbs against HIV-1 by use of Ganp^{Tg} *mice*

To apply this system for generating high-affinity Ab using *Ganp*^{Tg} mice, we studied whether high-affinity anti-HIV-1 mAbs with significant neutralization activity against virus infection could be generated by immunization with the V3 loop peptide (NL4-3) of HIV-1 gp120. Differential ELISA using plates coated with high and low doses of the V3 peptide initially identified hybridoma cells with relatively high-affinity mAbs from >6000 wells of (V3 peptide)-immunized *Ganp*^{Tg} and C57BL/6 mice. High-affinity clones were selected from each mouse strain. After further cloning, individual mAbs were purified and their affinities were measured using the BIAcore system. The mAbs from both mouse systems showed higher affinities in a range from $K_D = 2.81 \times 10^{-5}$ M to $\sim 5.67 \times 10^{-9}$ M. However, we could obtain extraordinarily higher affinity mAbs (V3-G2-10 and V3-G2-25; $K_D = 9.90 \times 10^{-11}$ M) from *Ganp*^{Tg} over the level that is generally not attainable by conventional methods of mAb preparation (20). The highest affinity mAbs (V3-W1-2 and V3-W1-8) from C57BL/6 mice were up to $K_D = 9.81 \times 10^{-8}$ M and 7.58×10^{-8} M. The high-affinity mAbs from *Ganp*^{Tg} used the same V_H region (V_HSm7) with the common mutation at T97I. suggesting that the T97I mutation contributed to an affinity increase against the V3 epitope (Fig. 4*A*). A binding assay involving HIV-1 envelope (NL4-3) gene-transfected cells was used to determine whether the mAb recognized the viral epitope. The binding activities to the transfectants were studied by flow cytometry as mean fluorescence intensity in comparison with the GFP-positivity as indicators of gene transfection. The mAbs (V3-G2-10, V3-G2-25, V3-W1-2, and V3-W1-8) showed higher binding activities to the virus epitope-expressing cells (Fig. 4*B*).

The neutralization activities of these anti-HIV-1 mAbs were examined using a CD4-LTR/β-galactosidase-transduced HeLa cell line that expresses high levels of human CD4 and contains a single integrated copy of a *β-galactosidase* gene under the control of a truncated HIV-1 LTR (13, 21). Neutralization activities of the two high-affinity mAbs (V3-G2-10 and V3-G2-25) were clearly detected at 0.5 μg/ml. which were more effective than those of mAbs (V3-W1-2 and V3-W1-8) from C57BL/6 (Fig. 4*C*). The simple comparison might indicate 50–100 times increase of affinity in the mAbs from *Ganp*^{Tg} mice. These mAbs with high-affinity Ag-binding and neutralization activities should be useful for clinical diagnostic purposes and analogous human mAbs might have therapeutic possibilities (22).

Discussion

Expression of GANP is required for generation of high-affinity Ab response in vivo, which was demonstrated by conditional targeting of *ganp* gene in B cells that caused apparent decrease in production of high-affinity Ab against NP-hapten, accompanied with the decreased frequency of high-affinity type mutation of W33L at the V_H186.2 in NP-binding IgG1$^+$ B cells (5). Several possibilities might be considered to explain the mechanism of GANP in generation of high-affinity BCR$^+$ B cells in vivo. GANP might be directly linked in genetic alteration, including *V* region dsDNA breaks occurring in B cell proliferation (23), SHM events in association with activation-induced cytidine deaminase (24), uracil DNA glycosylase (25), and error-prone DNA polymerases up-regulated in GC B cells (26), DNA recombination and repair mechanisms or rather involved in the selection of high-affinity BCR$^+$ B cells in the follicular dendritic cell network (27), and survival and maintenance of B cells with high-affinity type mutations throughout the immune response.

There are several possible mechanisms regarding the GANP function. Firstly, GANP might directly regulate generation of mutation frequency of the V_H region in GC B cells. The structure and expression of GANP indicated that GANP has two nuclear localization signal sequences (^{497}HKKK and ^{1345}PMKQKRR), two putative nuclear export signal sequences, and appears mostly in the nucleus but is also in the cytoplasm (our unpublished observation). The C-terminal region is capable of binding and acetylatiug with MCM3 of the MCM-complex that bears DNA helicase activity and is essential for DNA replication (28). In the N-terminal side, there is a putative RNA-associated region as the RNA recognition motif. The RNA-primase region and the RNA-binding activity might cooperate during the transcription at G_1 phase and introduce the alteration or the damage of the V_H region sequences during rapid cell proliferation in GCs. More interestingly, altered expression of

mouse SHD1 that has a homology to the central part of GANP (630–950 aa) caused an apparent cell cycle abnormality involving with centrosome duplication and M phase transition (29), which was also in accordance with the information of the association of *Saccharomyces* Sac3 with Cdc31/centrin (30). Loss of SHD1 caused an impairment of centrosome duplication, deregulated nuclear division, with disappearance of Mad2 expression in the prometaphase. Because mouse GANP is considered as a homologue of *Saccharomyces* Sac3 (31), GANP might be also involved in the centrosome duplication or the chromatin segregation during cell division. These observations suggested the involvement of GANP in either one or several mechanisms of gene transcription, DNA replication, and chromatin separation and cell division. Loss of GANP caused the increased apoptotic cells in GCs after immunization with TD-Ags (4), whereas the gain of function did not show obvious difference (data not shown). Second, these functions of GANP regions might be involved in the repair of DNA injuries occurring under a transcription-coupled mechanism or in the DNA replication phase. If this is the case, existence of GANP is critical for maintenance of DNA stability during the GC B cell stage that undergoes genetic alteration with frequent SHM of the V_H region and class switch recombination. Expression of GANP is necessary for the rescue of damaged GC B cells that potentially gain the high-affinity BCR. Third, additional function of GANP might be involved in generation or selection of high-affinity BCR$^+$ B cells in GCs. *Ganp*^{Tg} mice showed accelerated kinetics of GC formation (Fig. 1*F*), whereas B-*ganp*$^{-/-}$ mice showed retarded GC formation (4). Recently, Mirnics et al. (32) described that GANP is involved in downstream event(s) of Lyn. As Lyn is involved in CD40-mediated signal transduction (33) and Lyn-deficient mice showed lack of GCs (34), there might be functional interaction of CD40-mediated signaling with the GANP function involved in regulation of high-affinity B cells. The augmented anti-CD40 response of *Ganp*^{Tg} mice might support this notion, in which GANP is necessary for the rescue of high-affinity B cells during the selection in GCs. As a potential role of GANP in the selection process, GANP associates with a protein phosphatase component G5PR that associates with protein phosphatase 5 and protein phosphatase 2A (35). The complex of GANP with G5PR may regulate the other signaling pathways involved in cell survival mechanism or in regulation of BCR-mediated cell proliferation during maturation and selection of GC B cells. We have no definitive evidence to conclude the molecular mechanism at present but GANP is most likely a key molecule to elucidate the molecular mechanism in generation of high-affinity Ab in vivo.

To confirm the effect of GANP in generation of high-affinity Ab, we used a system to compare the affinity of the Abs at the monoclonal level by establishing the mAb-producing hybridomas. Affinity measurement with NP-hapten clearly demonstrated the high affinity of the mAbs generated from the *Ganp*^{Tg} mice. Sequence analyses of the *V* regions of individual mAb-producing hybridomas demonstrated that the high affinity was generated not only with increased SHM frequency in the $V_H186.2$ region but also with the noncanonical V_H region usage that was not seen in the control hybridomas.

The results of both the loss and gain of GANP expression caused adverse effects in generation of high affinity response, which confirmed that the GANP function is involved in generation of high-affinity Ab in vivo. Additionally, the high-affinity is generated with the genetic alteration of *V* region genes as increased SHM and the different *V* region usage. GANP function might be directly involved in the formation of high affinity V region of the GC B cells. GANP is not up-regulated in the nonimmunized condition and is not expressed in normal T cells at the similar level detected with anti-GANP mAb (3). We speculate that up-regulation of GANP is selective in the cells with frequent genetic alterations such as *V* region SHM and class switch recombination during rapid proliferation phase.

In summary, we have demonstrated that *Ganp*^{Tg} induces higher affinity Ab against TD-Ag in vivo, which was confirmed by BIAcore system with the purified mAbs against two model Ags of NP-hapten and the gp120 V3 peptide of HIV-1 by immunizing as TD-Ag. More importantly, the usage and the mutations of the V regions demonstrated that increased expression of GANP caused the genetic alteration of the *V* regions with increased mutations generating high affinity against TD-Ag in vivo. The results suggest that the *Ganp*^{Tg} mouse has an advantage in preparation of mAbs against various epitopes, for which conventional mice hardly generate high-affinity mAbs by the standard procedures. High-affinity mAbs generated this way show greater epitope binding constants and this binding is long-lasting as measured in vitro. It would be useful to generate high-affinity mAbs against various molecules, which can be applicable widely in the diagnostic and therapeutic purposes.

Acknowledgments

We appreciate Dr. Y. Takahashi and Dr. T. Takemori for helpful advice and Y. Kumamoto for technical assistance.

Disclosures

The authors have no financial conflict of interest.

References

1. MacLennan, I. C. M. 1994. Germinal centers. *Annu. Rev. Immunol. 12:117.*
2. Rajewsky, K. 1996. Clonal selection and learning in the antibody system. *Nature 381:751.*
3. Kuwahara, K., M. Yoshida, E. Kondo, A. Sakata, Y. Watanabe, E. Abe, Y. Kouno, S. Tomiyasu, S. Fujimura, T. Tokuhisa, et al. 2000. A novel nuclear phosphoprotein, GANP, is up-regulated in centrocytes of the germinal center and associated with MCM3, a protein essential for DNA replication. *Blood 95:2321.*
4. Kuwahara, K., S. Tomiyasu, S. Fujimura, K. Nomura, Y. Xing, N. Nishiyama, M. Ogawa, S. Imajoh-Ohmi, S. Izuta, and N. Sakaguchi. 2001. Germinal center-associated nuclear protein (GANP) has a phosphorylation-dependent DNA-primase activity that is up-regulated in germinal center regions. *Proc. Natl. Acad. Sci. USA 98:10279.*
5. Kuwahara, K., S. Fujimura, Y. Takahashi, N. Nakagata, T. Takemori, S. Aizawa, and N. Sakaguchi. 2004. Germinal center-associated nuclear protein contributes to affinity maturation of B cell antigen receptor in T cell-dependent responses. *Proc. Natl. Acad. Sci. USA 101:1010.*
6. Koike, M., Y. Kikuchi, A. Tominaga, S. Takaki, K. Akagi, J. Miyazaki, K. Yamamura, and K. Takatsu. 1995. Defective IL-5-receptor-mediated signaling in B cells of X-linked immunodeficient mice. *Int. Immunol. 7:21.*
7. Jonsson, U., L. Fagerstam, B. Ivarsson, B. Johnsson, R. Karlsson, K. Lundh, S. Lofas, B. Persson, H. Roos, I. Ronnberg, et al. 1991. Real-time biospecific interaction analysis using surface plasmon resonance and a sensor chip technology. *BioTechniques 11:620.*
8. Johnsson, B., S. Lofas, and G. Lindquist. 1991. Immobilization of proteins to a carboxymethyldextran-modified gold surface for biospecific interaction analysis in surface plasmon resonance sensors. *Anal. Biochem. 198:268.*
9. Karlsson, R., A. Michaelsson, and L. Mattsson. 1991. Kinetic analysis of monoclonal antibody-antigen interactions with a new biosensor based analytical system. *J. Immunol. Methods 145:229.*
10. Furukawa, K., A. Akasako-Furukawa, H. Shirai, H. Nakamura, and T. Azuma. 1999. Junctional amino acids determine the maturation pathway of an antibody. *Immunity 11:329.*
11. Chen, J., P. Borden, J. Liao, and E. A. Kabat. 1992. Variable region cDNA sequences of three mouse monoclonal anti-idiotypic antibodies specific for anti-$\alpha_{1\to6}$ dextran with groove- or cavity-type combining sites. *Mol. Immunol. 29:1121.*
12. Wei, C., R. Zeff, and I. Goldschneider. 2000. Murine pro-B cells require IL-7 and its receptor complex to up-regulate IL-7Rα, terminal deoxynucleotidyltransferase, and cμ expression. *J. Immunol. 164:1961.*
13. Kimura, T., K. Yoshimura, K. Nishihara, Y. Maeda, S. Matsumi, A. Koito, and S. Matsushita. 2002. Reconstitution of spontaneous neutralizing antibody response against autologous human immunodeficiency virus during highly active antiretroviral therapy. *J. Infect. Dis. 185:53.*
14. Reed, L. J., and H. Muench. 1938. A simple method of estimating fifty percent end points. *Am. J. Hyg. 27:493.*
15. Jacob, J., G. Kelsoe, K. Rajewsky, and U. Weiss. 1991. Intracional generation of antibody mutants in germinal centres. *Nature 354:389.*
16. Jacob, J., J. Przylepa, C. Miller, and G. Kelsoe. 1993. In situ studies of the primary immune response to (4-hydroxy-3-nitrophenyl)acetyl. III. The kinetics of

V region mutation and selection in germinal center B cells. *J. Exp. Med. 178:1293.*

17. Cumano, A., and K. Rajewsky. 1986. Clonal recruitment and somatic mutation in the generation of immunological memory to the hapten NP. *EMBO J. 5:2459.*
18. Allen, D., T. Simon, F. Sablitzky, K. Rajewsky, and A. Cumano. 1988. Antibody engineering for the analysis of affinity maturation of an anti-hapten response. *EMBO J. 7:1995.*
19. French, D. L., R. Laskov, and M. D. Scharff. 1998. The role of somatic hypermutation in the generation of antibody diversity. *Science 244:1152.*
20. Poignard, P., T. Fouts, D. Naniche, J. P. Moore, and Q. J. Sattentau. 1996. Neutralizing antibodies to human immunodeficiency virus type-1 gp120 induce envelope glycoprotein subunit dissociation. *J. Exp. Med. 183:473.*
21. Kimpton, J., and M. Emerman. 1992. Detection of replication-competent and pseudotyped human immunodeficiency virus with a sensitive cell line on the basis of activation of an integrated β-galactosidase gene. *J. Virol. 66:2232.*
22. Matsushita, S., H. Maeda, K. Kimachi, Y. Eda, Y. Maeda, T. Murakami, S. Tokiyoshi, and K. Takatsuki. 1992. Characterization of a mouse/human chimeric monoclonal antibody (C2H) to a principal neutralizing domain of the human immunodeficiency virus type 1 envelope protein. *AIDS Res. Hum. Retroviruses 8:1107.*
23. Wu, X., J. Feng, A. Komori, E. C. Kim, H. Zan, and P. Casali. 2003. Immunoglobulin somatic hypermutation: double-strand DNA breaks, AID and error-prone DNA repair. *J. Clin. Immunol. 23:235.*
24. Honjo, T., K. Kinoshita, and M. Muramatsu. 2002. Molecular mechanism of class switch recombination: linkage with somatic hypermutation. *Annu. Rev. Immunol. 20:165.*
25. Storb, U., and J. Stavnezer. 2002. Immunoglobulin genes: generating diversity with AID and UNG. *Curr. Biol. 12:R725.*
26. Jacobs, H., and L. Bross. 2001. Towards an understanding of somatic hypermutation. *Curr. Opin. Immunol. 13:208.*
27. van Eijk, M., T. Defrance, A. Hennino, and C. de Groot. 2001. Death-receptor contribution to the germinal-center reaction. *Trends Immunol. 22:677.*
28. Bailis, J. M., and S. L. Forsburg. 2004. MCM proteins: DNA damage, mutagenesis and repair. *Curr. Opin. Genet. Dev. 14:17.*
29. Khuda, S. E., M. Yoshida, Y. Xing, T. Shimasaki, M. Takeya, K. Kuwahara, and N. Sakaguchi. 2004. The *Sac3* homolngue *shd1* is involved in mitotic progression in mammalian cells. *J. Biol. Chem. 279:46182.*
30. Fischer, T., S. Rodriguez-Navarro, G. Pereira, A. Racz, E. Schiebel, and E. Hurt. 2004. Yeast centrin Cdc31 is linked to the nuclear mRNA export machinery. *Nat. Cell Biol. 6:840.*
31. Bauer, A., and R. Kölling. 1996. Characterization of the SAC3 gene of *Saccharomyces cerevisiae*. *Yeast 12:965.*
32. Mimics, Z. K., E. Caudell, Y. Gao, K. Kuwahara, N. Sakaguchi, T. Kurosaki, J. Burnside, K. Mimics, and S. J. Corey. 2004. Microarray analysis of Lyn-deficient B cells reveals germinal center-associated nuclear protein and other genes associated with the lymphoid germinal center. *J. Immunol. 172:4133.*
33. Ren, C. L., T. Morio, S. M. Fu, and R. S. Geha. 1994. Signal transduction via CD40 involves activation of *lyn* kinase and phosphatidylinositol-3-kinase, and phosphorylation of phospholipase Cγ2. *J. Exp. Med. 179:673.*
34. Nishizumi, H., I. Taniuchi, Y. Yamanashi, D. Kitamura, D. Ilic, S. Mori, T. Watanabe, and T. Yamamoto. 1995. Impaired proliferation of peripheral B cells and indication of autoimmune disease in *lyn*-deficient mice. *Immunity 3:549.*
35. Kono, Y., K. Maeda, K. Kuwahara, H. Yamamoto, E. Miyamoto, K. Yoneczawa, K. Takagi, and N. Sakaguchi. 2002. MCM3-binding GANP DNA-primase is associated with a novel phosphatase component GSPR. *Genes Cells 7:821.*